Antarct. Meteorite Res., **13**, 19–38, 2000

Geochemical and isotopic evidence bearing on the origin of large, igneous-textured inclusions in ordinary chondrites

Alex Ruzicka*, Gregory A. Snyder and Lawrence A. Taylor

Planetary Geosciences Institute, Department of Geological Sciences, University of Tennessee, Knoxville TN 37996, U.S.A.

Abstract: Geochemical and isotopic data for large, igneous-textured inclusions in ordinary chondrites suggest that the inclusions formed by the melting of diverse precursors, and that various inclusions had different origins. Some inclusions were metasomatized (chemically altered) and metamorphosed, and many appear to have degassed argon in late shock events. The inclusions can be subdivided into two chemical groups, Na-rich (Na/Al >0.35 at.) and Na-poor (≤ 0.35), which may have originated in different ways.

The major- and trace-element abundances of Na-rich inclusions are best explained by these inclusions having formed by the shock-melting of ordinary chondrites, often accompanied by loss of FeNi-metal and sulfide and by preferential melting and accumulation of an albitic feldspar component. In contrast, there is no evidence that shock-melting was involved in the formation of Na-poor inclusions, which have compositions that were largely controlled by vapor-fractionation processes. It is suggested that the precursors to Na-poor inclusions consisted of mixtures of vapor-fractionated materials in a system of condensed phases that chemically resembled CI-chondrites, except for being depleted in volatile-lithophile elements and in metal and sulfide.

Sodium-poor inclusions can be subdivided into two types, Trend A and Trend B, which differ in their trace-element characteristics, in the nature of their compositional variations, and in their inferred precursors. Trend A Na-poor inclusions are enriched in refractory elements, and could have formed by the melting of mixtures containing a chondritic (CI-like) component and a refractory (Al-rich, CAI-like) component. Trend B Na-poor inclusions are enriched in elements of intermediate volatility (Si) and appear to have formed from precursors that lost both a refractory (Mg-rich, olivine-rich) and a volatile component. The precursors to these inclusions could have been produced by the removal of an olivine-rich condensate during fractional condensation, or by the condensation of Si-rich gases during fractional vaporization.

1. Introduction

The existence of large, igneous-textured inclusions in ordinary chondrites (*e.g.*, Bridges and Hutchison, 1997) has important implications for processes that affected

* Now at: Department of Geology, Portland State University, Portland, OR 97207-0751, U.S.A.; and Portland Community College, P.O. Box 19000, Portland, OR 97280-0990, U.S.A. E-mail: aruzicka @uswest.net.

ordinary chondrites and may bear on the origin of chondrules, which remain enigmatic despite many decades of study. Besides being larger (up to 4 cm in diameter) compared to most chondrules, the inclusions are typically depleted in FeNi-metal and sulfide compared to the host-rocks and to many chondrules (Ruzicka *et al.*, 1998). In hand-specimen, they appear either light- or dark-colored. In this study, "large inclusions" are defined to be objects $\geq$0.4 cm in diameter which show textural evidence of having largely crystallized from a melt. It should be noted that large chondrules also fit this definition, so that the inclusions considered here could represent unusually big chondrules.

Various melting processes for the large inclusions have been proposed. These include (1) shock-melting of ordinary chondrites with accompanying loss of metal and sulfide (*e.g.*, Dodd and Jarosewich, 1976; Fodor and Keil, 1976a, b; Keil *et al.*, 1980; Boctor *et al.*, 1982), (2) chondrule formation involving unusually large volumes of melt production (Binns, 1967; Weisberg *et al.*, 1988), and (3) igneous differentiation occurring within chondrite parent bodies (Hutchison *et al.*, 1988; Ruzicka *et al.*, 1995; Bridges *et al.*, 1995).

Ruzicka *et al.* (1998) subdivided large inclusions in ordinary chondrites into two chemical types: Na-rich and Na-poor; and into two textural-shape types: mega-chondrules and large, igneous textured clasts. Sodium-rich inclusions have generally chondritic or superchondritic abundances of volatile-elements (Mn, K, Na) and relatively high Na/Al values, whereas Na-poor inclusions have sub-chondritic abundances of Na and lower Na/Al values. Mega-chondrules display textural evidence (partly-to-wholly curved surfaces, radial variations in textures) of having crystallized as large, free-floating droplets, whereas large, igneous textured clasts have irregular margins and appear to be fragments of still-larger objects. The textures of the inclusions are diverse (barred-olivine, barred-olivine-pyroxene, poikilitic, granular, microporphyritic, radial-pyroxene, cryptocrystalline, clast-laden) and are largely uncorrelated with chemical type, although barred textures are most common for mega-chondrules. Ruzicka *et al.* (1998) suggested that Na-rich inclusions formed by shock-melting, and that Na-poor inclusions formed by the melting of vapor-fractionated mixtures.

Here, we synthesize geochemical and isotopic data for igneous-textured inclusions in ordinary chondrites $\geq$0.4 cm across that have been studied to date and reassess the origins of the inclusions. Based on an expanded database, the data support the conclusion of Ruzicka *et al.* (1998) that the inclusions can be subdivided into two basic chemical types which may have originated differently.

2. Database

Table 1 provides a listing of the large ($>$4 mm), igneous-textured inclusions that have been described in ordinary chondrites. This table briefly describes the inclusions, identifies the host rocks in which the inclusions are found, and assigns a name (where not previously designated) and chemical group to each inclusion. In addition, Table 1 summarizes the analytical techniques that were used to obtain the

Table 1. Large (≥4 mm-diameter), igneous-textured inclusions in ordinary chondrites.

Inclusion	Chemical Group*	Description¶	Host Rock	Method†	Reference§
Pa-1	Na-rich	ol microporphyry "macrochondrule"	Parnallee (LL3)	a	[1]
OG-1	Na-rich	fine-grained granulitic fragment	Oro Grande (H5)	b	[2]
PV2	Na-poor	ol microporphyry clast	Plainview (H5) breccia	b	[3]
PV4	Na-rich	ol microporphyry clast	Plainview (H5) breccia	b	[3]
PV7b	Na-rich	ol microporphyry clast	Plainview (H5) breccia	b	[3]
Ev-1	Na-rich	spinifex-textured lithic fragment	Eva (H5)	b	[4, 30]
d5	Na-rich	ol microporphyry "xenolith"	St. Mesmin (L3-7/H6)	a	[5]
AC-1	Na-rich	"clast-laden melt-rock fragment"	Adams County (H5)	b,c	[6, 7]
PV-A	Na-rich	"poikilitic melt-rock fragment"	Plainview (H5) breccia	c,d,e	[8]
Gr-1	Na-rich	"granulitic fragment"	Grier (b) (L5)	f	[9]
Bo-2	Na-poor	poikilitic/granular lithic fragment	Bovedy (L3/4)	b,c,e	[10]
PdI-1	Na-rich	"spinifex-textured clast"	Pampa del Infierno (L6)	b	[11]
PdI-2	Na-rich	"granulitic clast"	Pampa del Infierno (L6)	b	[11]
Ro-1	Na-rich	variolitic-to-microporphyritic ol	Romero (H3/4)	b	[12]
DT4	Na-rich	"poikilitic melt-rock clast"	Dimmitt (H3-5/LL5)	c,e	[13]
Et-2	Na-rich	ol microporphyry clast	Etter (L5)	b	[14]
JC-1	Na-rich	ol-px microporphyry clast	Johnson City (L6)	b	[14]
LC-1	Na-rich	ol-px microporphyry clast	Lincoln County (L6)	b,c	[14]
Y75-1	Na-rich	"dunite-troctolite clast"	Y-75097 (L6)	a,c,d,e,f,g,h	[15-23]
Y79-1	Na-rich	"troctolitic clast"	Y-793241 (L6)	a,c,d,e,h	[16-19, 21-25]
Y79-2	Na-rich	"harzburgitic clast"	Y-794046 (H5)	a,c,d,e,h,g	[18, 21-26]
Bar-1	Na-poor	"troctolitic pebble"	Barwell (L6)	b,c,d,e	[27]
Bo-1	Na-poor	silica-rich pyroxenite clast	Bovedy (L3/4)	e,g	[28]
CB8	Na-poor	silica-rich pyroxenite clast	Parnallee (LL3)	e,g,h	[29]
Jl-1	Na-poor	ol microporphyry clast	Julesburg (L3)	g	[30]
Jl-2	Na-poor	barred ol-px megachondrule	Julesburg (L3)	g	[30]
Jl-3	Na-poor	barred ol-px megachondrule	Julesburg (L3)	g	[30]
Jl-4	Na-poor	granular ol lithic clast	Julesburg (L3)	g	[30]
Jl-5	Na-rich	ol vitrophyre clast	Julesburg (L3)	g	[30]
Jl-6	Na-poor	barred ol-px clast	Julesburg (L3)	g	[30]
Jl-7	Na-rich	clast-laden melt-rock fragment	Julesburg (L3)	g	[30]
Jl-9	Na-poor	barred ol megachondrule	Julesburg (L3)	g	[30]
Jl-10	Na-poor	silica-rich pyroxenite clast	Julesburg (L3)	g	[30]
Jl-11	Na-poor	ol-px clast	Julesburg (L3)	g	[30]
Jl-12	Na-poor	silica-rich radial px megachondrule	Julesburg (L3)	g	[30]
Jl-13	Na-poor	barred ol-px megachondrule	Julesburg (L3)	g	[30]
Jl-14	Na-poor	granular ol-rich clast	Julesburg (L3)	g	[30]
Jl-15	Na-poor	barred ol megachondrule	Julesburg (L3)	g	[30]
Jl-16	Na-poor	granular/poikilitic clast	Julesburg (L3)	g	[30]
Jl-17	Na-rich	cryptocrystalline megachondrule	Julesburg (L3)	g	[30]
Jl-18	Na-poor	barred ol megachondrule	Julesburg (L3)	g	[30]
Jl-19	Na-poor	ol microporphyry clast	Julesburg (L3)	g	[30]
Jl-20	Na-poor	px-rich poikilitic clast	Julesburg (L3)	g	[30]
Ho-1	Na-poor	barred ol-px megachondrule	Homestead (L5)	g	[30]
Et-1	Na-rich	ol microporphyry clast	Etter (L5)	g	[30]
Gu-1	Na-rich	ol microporphyry clast	Gunlock (L3)	g	[30-32]
Ca-1	Na-rich	barred ol megachondrule	Carraweena (L3)	g	[30, 31]
LEW-1	Na-poor	barred/poikilitic/granular clast	LEW-86018 (L3)	c,g	[33]

* Na-poor: Na/Al ≤0.35 atomic, Na-rich: Na/Al > 0.35 atomic. ¶ ol = olivine, px = pyroxene. † Technique used for bulk chemical or isotopic analysis: a = wet-chemistry, b = defocussed electron microprobe analysis, c = instrumental-neutron-activation-analysis, d = radiochemical-neutron-activation-analysis, e = mass-spectrometric methods, f = electron microprobe analysis of fused beads, g = modal reconstruction based on electron microprobe, h = isotope dilution. § References: [1] Binns (1967). [2] Fodor *et al.* (1972). [3] Fodor and Keil (1976a). [4] Fodor *et al.* (1976b). [5] Dodd and Jarosewich (1976). [6] Fodor *et al.* (1974). [7] Fodor *et al.* (1980). [8] Keil *et al.* (1980). [9] Fredriksson *et al.* (1981). [10] Rubin *et al.* (1981). [11] Boctor *et al.* (1982). [12] Graham (1983). [13] Rubin *et al.* (1983a). [14] Rubin *et al.* (1983b). [15] Yanai *et al.* (1983). [16] Prinz *et al.* (1984). [17] Nakamura *et al.* (1984). [18] Yanai and Kojima (1987), see plates 51-52 (Y75-1), 309-313 (Y79-1) and 378-380 (Y79-2). [19] Mayeda *et al.* (1987). [20] Warren and Kallemeyn (1989). [21] Yanai and Kojima (1993). [22] Nagao (1994). [23] Sack *et al.* (1994). [24] Nakamura *et al.* (1994). [25] Fukuoka (1993). [26] Fujimake *et al.* (1993). [27] Hutchison *et al.* (1988). [28] Ruzicka *et al.* (1995). [29] Bridges *et al.* (1995). [30] Ruzicka *et al.* (1998). [31] Weisberg *et al.* (1988). [32] Prinz *et al.* (1988). [33] Ruzicka *et al.* (1999).

data. Mineral-chemical, textural, and size data for the inclusions can be found in the original references listed in Table 1 and are not repeated here. All of the geochemical and isotopic data discussed in this paper are derived from the sources listed in Table 1. Compared to Ruzicka *et al.* (1998), the database for this paper includes roughly twice as many analyses for major elements, as well as trace-element and isotopic data which were not considered in the earlier work.

3. Results and discussion

3.1. Major-element abundances

Major-element data provide evidence for two chemical groups among the inclusions, and provide clues as to how the inclusions may have formed. Data are summarized in Figs. 1, 2, 3, and 4.

Na-Al abundance systematics

The chemical parameter that best distinguishes different chemical groups of the inclusions is the Na/Al abundance ratio. Evidence for two populations of inclusions is provided by a bimodal distribution in Na/Al values (Fig. 1): many inclusions have Na/Al~0.1 (atomic), and most of the remaining inclusions have Na/Al values spread over ~0.35–0.85. The former inclusions are classified as "Na-poor", the latter as "Na-rich". The cut-off between the two groups is placed at Na/Al= 0.35, based on other evidence (summarized below) that inclusions with Na/Al values less than this form a chemically coherent group.

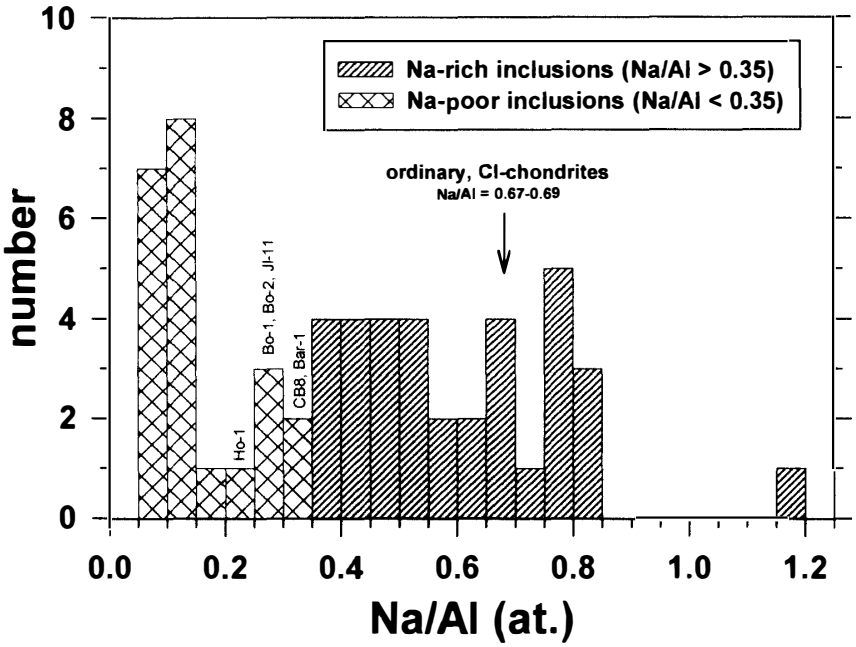

Fig. 1. Histogram showing the frequency of inclusions having a given bulk Na/Al abundance ratio. Multiple determinations of Na/Al were made for some inclusions (e.g., Y75-1); these were not averaged but are plotted individually. Average Na/Al abundance ratios for ordinary and CI-chondrites are from Jarosewich (1990) and Anders and Grevesse (1989), respectively. Other data sources are given in Table 1.

Some Na-poor inclusions (Ho-1, Jl-11, Bar-1) with relatively high Na/Al values (~0.20–0.35) appear to have had lower Na abundances prior to a metasomatic event that enriched the margins of the inclusions in sodium and other volatile elements (Hutchison *et al.*, 1988; Ruzicka *et al.*, 1998). In contrast, there is no evidence for the reverse process (an outflux of Na) in any of the inclusions. Thus, it is conceivable that some Na-rich inclusions may represent Na-poor inclusions that were modified by metasomatism, but there is no evidence for the reverse being true.

Sodium-rich and -poor inclusions form two different trends on an Na *vs.* Al diagram, although Na and Al abundances appear to co-vary for both types of inclusions (Fig. 2). Most Na-rich inclusions have Na and Al abundances similar to those in ordinary chondrite silicate, but some (*e.g.*, Jl-5, OG-1) have much higher abundances of both elements and are relatively feldspathic (Fig. 2). In contrast, Na-poor inclusions typically have subchondritic Na abundances (Fig. 2).

The compositions of Na-rich inclusions overlap the range of compositions shown by melt-pocket-glasses (Fig. 2). These glasses were undoubtedly formed by shock-induced, localized melting (*e.g.*, Stöffler *et al.*, 1991). The compositional similarity between melt-pocket glasses and the Na-rich inclusions implies that Na-rich inclusions could have formed by shock-melting. As is the case for

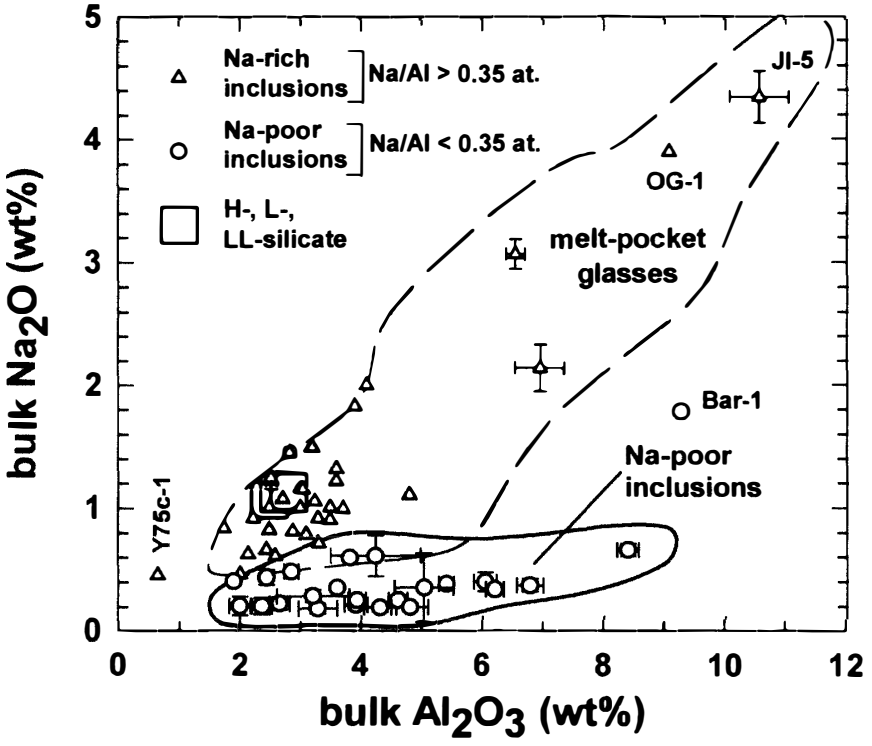

Fig. 2. Bulk soda and alumina abundances in large, igneous-textured inclusions, compared to melt-pocket glasses in L6 chondrites and average H-, L- and LL-chondrite silicate. Melt-pocket glass data are from Dodd and Jarosewich (1982) and Dodd et al. (1983); H/L/LL chondrite data are from Jarosewich (1990). Other data sources are given in Table 1.

feldspathic melt-pocket glasses (Dodd and Jarosewich, 1982; Dodd *et al.*, 1983), feldspathic Na-rich inclusions could have formed by the shock-induced, preferential melting and accumulation of a feldspar component.

One Na-rich inclusion (Y75-1) has a radial (core-mantle) structure including a core rich in olivine and phosphate, and a mantle containing little phosphate and more feldspar (Yanai *et al.*, 1983; Prinz *et al.*, 1983; Nakamura *et al.*, 1984; Warren and Kallemeyn, 1989). An analysis of the core of this object (designated Y75c-1) yields a distinctly low Al abundance (Fig. 2), but this is unrepresentative of the inclusion as a whole.

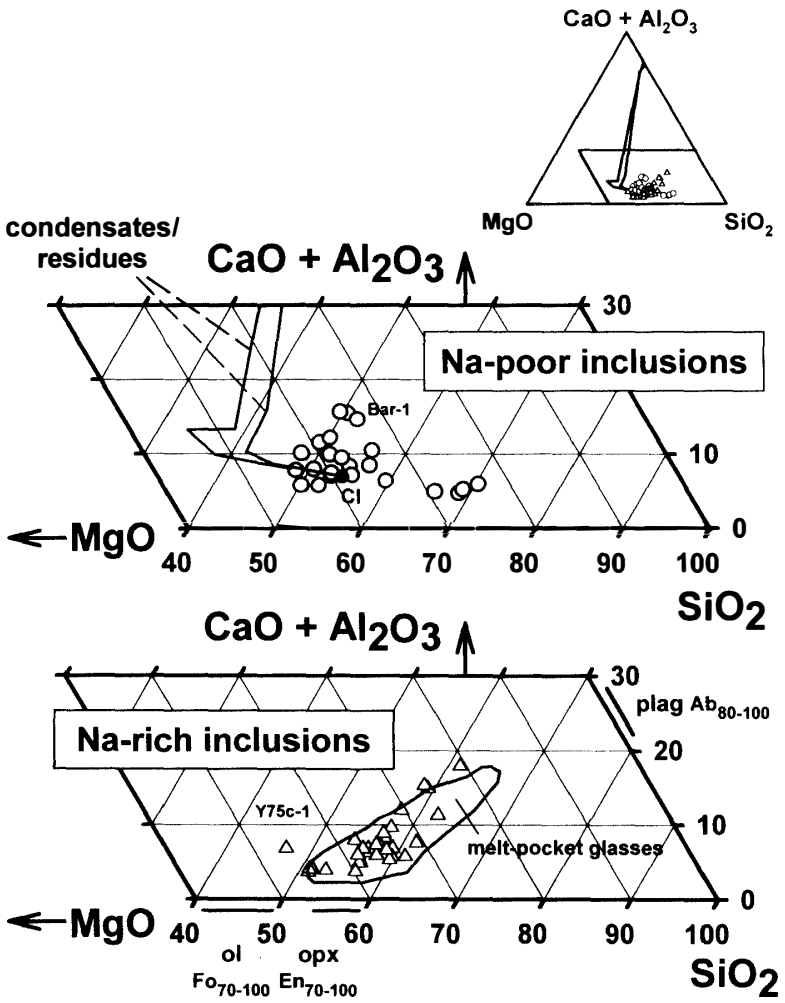

Fig. 3. Bulk compositions of inclusions projected on a ($CaO+Al_2O_3$)-MgO-SiO_2 ternary diagram, compared to melt-pocket glasses and to the calculated compositions of equilibrium condensates or residues in a generally chondritic system. The latter calculations were performed using the PHEQ program (Wood and Hashimoto, 1993) and assumed a system with CI-chondrite proportions of cationic elements, a total gas pressure of 10^{-5} bar, and two extreme values for "dust/gas" ratios (cosmic to 10000×dust-enriched, as defined by Wood and Hashimoto, 1993). Melt-pocket glass data are from Dodd and Jarosewich (1982) and Dodd et al. (1983); the CI-chondrite composition is from Anders and Grevesse (1989). Other data sources are as in Table 1.

Ca-Al-Mg-Si abundance systematics

Sodium-rich and -poor inclusions can also be distinguished based on the abundances of relatively involatile elements such as Ca, Al, Mg, and Si. Figure 3 shows the compositions of the inclusions projected on a portion of a $(CaO+Al_2O_3)$–MgO–SiO_2 (CMAS) ternary diagram. Once again, Na-poor and Na-rich inclusions form different clusters or trends, although the compositions overlap (Fig. 3). Most Na-rich inclusions have compositions that cluster around that of ordinary chondrite silicate, but some have either more or less of an albitic feldspar component (Fig. 3). In the CMAS projection, the compositions of Na-rich inclusions substantially overlap that of melt-pocket-glasses (Fig. 3). This similarity strengthens the idea that Na-rich inclusions formed by shock-melting of ordinary chondrite material.

In contrast, the compositions of Na-poor inclusions do not have compositions controlled by variations in feldspar abundance alone (Fig. 3). Inclusion Bar-1 appears to fall within the range shown by other Na-poor inclusions (Fig. 3), which supports the classification of Bar-1 as an Na-poor inclusion that experienced some secondary Na-enrichment. Other Na-poor inclusions (Bo-1, CB8, Jl-10, Jl-12) have silica-rich compositions that are distinctly unlike that of CI-chondrites or Na-rich inclusions (Fig. 3).

Chemical differences not only between Na-rich and Na-poor inclusions, but also between different types of Na-poor inclusions, can be distinguished in a plot of the abundance ratio of Mg/Al and Si/Al (Fig. 4). In Fig. 4, refractory material similar to Type B Ca-Al-rich inclusions (CAIs) plots near the origin, whereas plagioclase plots on the abscissa close to the origin. The Mg/Si abundance ratio (and olivine/pyroxene ratio) increases from lower right to upper left.

In terms of Si/Al and Mg/Al abundance ratios, the compositions of most Na-rich inclusions form a trend that can be described as a mixing line extending between an ordinary chondrite (H/L/LL) composition and feldspar (Fig. 4). This suggests that the compositional variation in Na-rich inclusions is controlled primarily by variations in a normative feldspar component. In Na-rich inclusions, variations in normative feldspar are manifested by variations in the modal abundance of either albitic plagioclase or of albitic glass.

Among Na-rich inclusions, four data points with relatively high Mg/Al and low Si/Al lie off the feldspar-variation line (Fig. 4); these include two analyses of inclusion Y75-1, and one each of Jl-7 and Y79-1. Both Y75-1 and Y79-1 have Na-enriched margins (Prinz *et al.*, 1984; Yanai and Kojima, 1993) and appear to have been Na-metasomatized; they may be modified Na-poor inclusions. Inclusion Jl-7 is clast-laden (Table 1) and may have obtained a relatively high proportion of olivine during the brecciation process apparently involved in its formation.

Sodium-poor inclusions form two trends (A and B) in Fig. 4 that intersect near the composition of CI-chondrites. The approximate intersection of these two trends near the CI-chondrite composition implies that both Trend A and B inclusions could have been derived, in part, from a precursor with CI-like proportions of Mg, Al, and Si. However, such a precursor would have to have been depleted in volatile elements, such as Na. The two trends for Na-poor inclusions appear to be

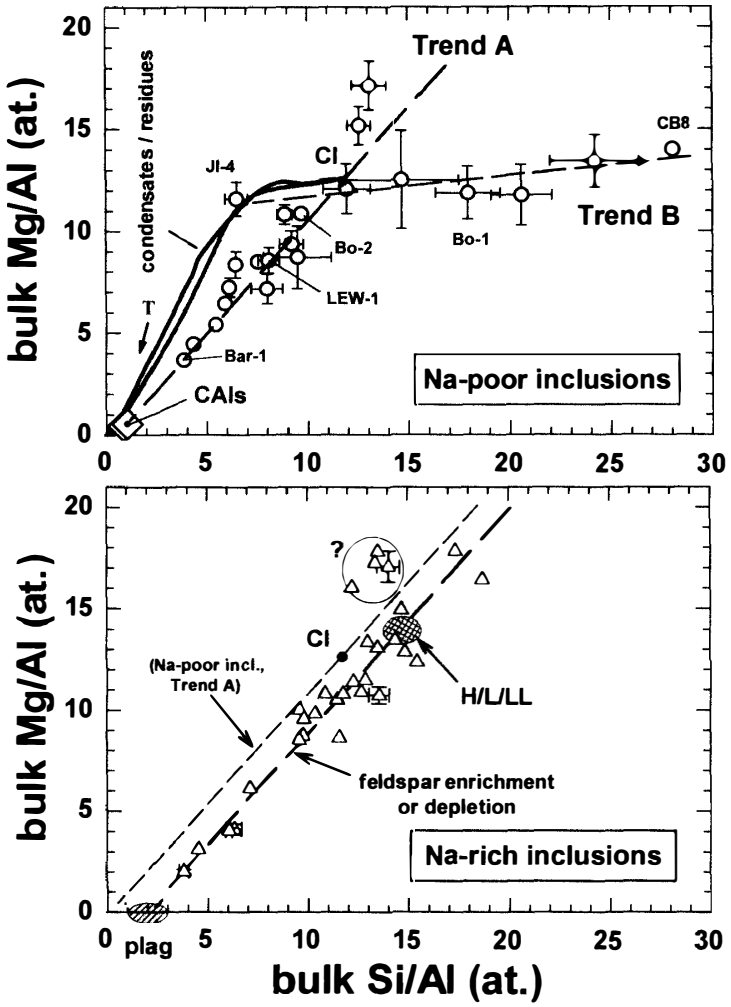

Fig. 4. Mg/Al and Si/Al abundance ratios in large inclusions compared to a feldspar-variation trend, the calculated compositions of equilibrium condensates or residues in a system with CI-chondrite composition, and average Type B Ca-Al-rich inclusions (CAIs). The CAI data are from MacPherson et al. (1988); other data sources, and the details associated with the condensate/residue compositions, are as in Fig. 3. T=temperature.

systematically related to the compositional trend of equilibrium condensates or residues in a system with CI-like proportions of Mg, Al, and Si (Fig. 4). As discussed below, the two compositional trends (A & B) for Na-poor inclusions can be explained by the mixing of vapor-fractionated materials.

The Na-poor inclusions along Trend A are characterized by a relatively constant Mg/Si ratio and variable Al abundances (Fig. 4). The Mg/Si abundance ratios of these inclusions are similar to that in CI-chondrites (Fig. 4). These inclusions could have formed by the melting of a CI-like precursor that contained variable proportions of an Al-rich component similar to CAIs (Fig. 4). On the basis of Fig. 4, it cannot be determined whether the Al-rich component is CAI-like or more similar to anorthitic plagioclase, but trace-element data (discussed below) suggest that the Al-component is rich in other refractory elements such as rare-

earth-elements, and that it is more similar to CAIs.

Most Trend A inclusions have lower Mg/Al and Si/Al values than CI-chondrites, and they are, therefore, enriched in a refractory component. The compositions of these inclusions cannot be explained by equilibrium condensation or vaporization processes alone, as their compositions do not match the calculated trends for equilibrium condensates in chondritic systems (*e.g.*, Fig. 4). Instead, the compositions of Trend A Na-poor inclusions are best explained by the melting of pre-existing mixtures of vapor-fractionated materials, which included a high-temperature (CAI-like) component, and a low-temperature or "largely condensed" (CI-like) component. Alternatively, the Trend A inclusions could have formed by grossly non-equilibrium vapor-fractionation processes.

Trend B Na-poor inclusions form a completely different trend, with large variations in Mg/Si ratio. These inclusions range from olivine-rich inclusion Jl-4, to olivine-free and tridymite-bearing inclusions Bo-1, Jl-10, Jl-12, and CB8 (Fig. 4). Inclusion Jl-4 has a composition which corresponds to that of the most olivine-rich condensate or residue expected in a system (gas + condensed material) with an overall composition similar to CI-chondrites. The precursors to the silica-rich inclusions of Trend B (Bo-1, etc.) could have formed in one of two ways, either (1) as fractional condensates produced by removing olivine-rich condensates during condensation, or (2) as condensates from the silica-rich gases produced by fractional vaporization of CI-like material. The silica-rich compositions of these inclusions can also be obtained by multi-stage igneous differentiation processes operating on chondritic material (Ruzicka *et al.*, 1995; Bridges *et al.*, 1995). However, considering all available major- and trace-element data (see Section 3.2), the compositions of these and other Na-poor inclusions are more simply explained by vapor-fractionation processes including some combination of vaporization and condensation.

3.2. Trace-element abundances

Trace-element data for the inclusions are illustrated in Figs. 5 and 6. Figure 5 shows CI-normalized abundances, with elements arranged according to volatility and geochemical tendency (lithophile and siderophile/chalcophile). Rare-earth-element (REE) plots are shown in Fig. 6. In the following discussion, it is convenient to split the inclusions into three groups based on their trace-element characteristics: typical Na-poor, typical Na-rich, and fractionated.

Typical Na-poor inclusions

Na-poor inclusions (LEW-1, Bo-2, Bo-1, CB8) are progressively depleted in elements more volatile than Si (Fig. 5a). This suggests that these inclusions were affected by vapor-fractionation processes. Rare-earth-element patterns for these inclusions are relatively flat, although a positive Eu anomaly occurs for CB8 and possibly LEW-1 (Fig. 6a).

Trend A and B Na-poor inclusions differ in that Trend B inclusions have an abundance maxima for elements of intermediate volatilities (Ca to Si), whereas Trend A inclusions are most enriched in elements more refractory than Ca (Fig.

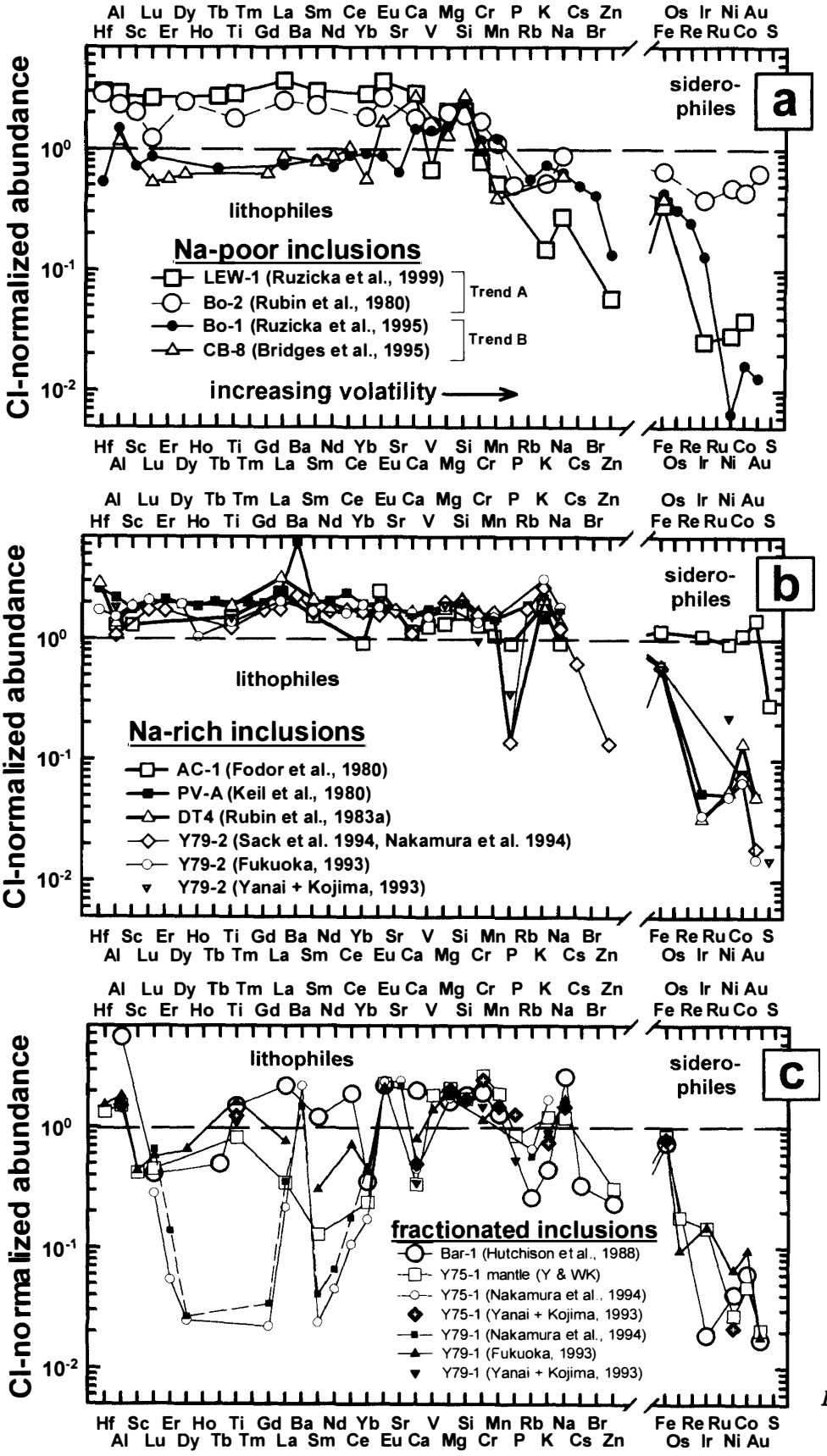
Al Lu Dy Tb Tm La Sm Ce Eu Ca Mg Cr P K Cs Zn
Hf Sc Er Ho Ti Gd Ba Nd Yb Sr V Si Mn Rb Na Br
Os Ir Ni Au
Fe Re Ru Co S
Cl-normalized abundance
siderophiles
a
lithophiles
Na-poor inclusions
LEW-1 (Ruzicka et al., 1999)
Bo-2 (Rubin et al., 1980)
Bo-1 (Ruzicka et al., 1995)
CB-8 (Bridges et al., 1995)
Trend A
Trend B
increasing volatility
b
Na-rich inclusions
AC-1 (Fodor et al., 1980)
PV-A (Keil et al., 1980)
DT4 (Rubin et al., 1983a)
Y79-2 (Sack et al. 1994, Nakamura et al. 1994)
Y79-2 (Fukuoka, 1993)
Y79-2 (Yanai + Kojima, 1993)
c
fractionated inclusions
Bar-1 (Hutchison et al., 1988)
Y75-1 mantle (Y & WK)
Y75-1 (Nakamura et al., 1994)
Y75-1 (Yanai + Kojima, 1993)
Y79-1 (Nakamura et al., 1994)
Y79-1 (Fukuoka, 1993)
Y79-1 (Yanai + Kojima, 1993)

Fig. 5.

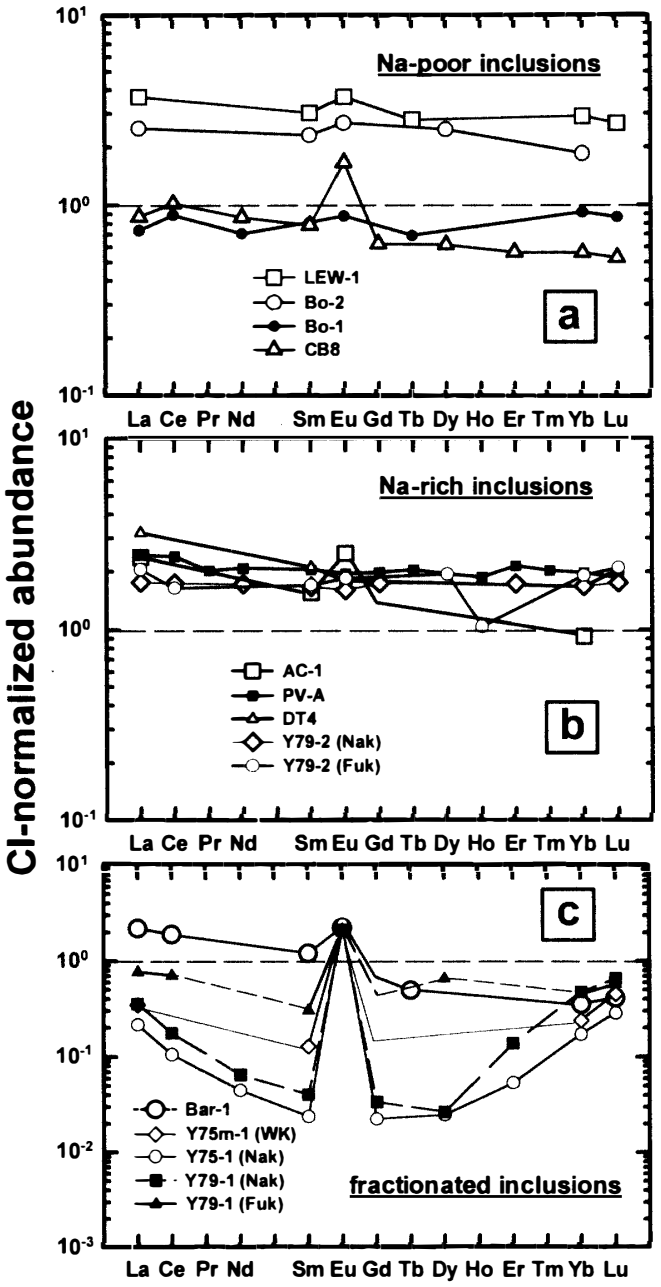

Fig. 6. Rare-earth-element diagrams for (a) typical Na-poor inclusions, (b) typical Na-rich inclusions, and (c) fractionated inclusions. The average CI-chondrite abundances of Anders and Grevesse (1989) were used for normalization. Data sources: Y79-2 (NAK) = Nakamura et al. (1994); Y79-2 (Fuk) = Fukuoka (1993); Y75m-1 (WK) = Warren and Kallemeyn (1989); Y79-1 (Nak) = Nakamura et al., (1994); Y79-1 (Fuk) = Fukuoka (1993); and as in Table 1.

5a). Refractory trace-element abundances range from ~2–4×CI-chondrites in Trend A inclusions LEW-1 and Bo-2, to ~0.5–1×CI-chondrites in Trend B inclusions Bo-1 and CB8 (Fig. 5a, 6a).

In general, Trend A inclusions have trace-element abundances suggestive of

Fig. 5 (opposite). CI-normalized abundances of elements in (a) typical Na-poor inclusions, (b) typical Na-rich inclusions, and (c) fractionated inclusions. Elements are arranged in the order of increasing volatility from left to right for lithophile and siderophile/chalcophile elements separately. The average CI-chondrite abundances of Anders and Grevesse (1989) were used for normalization. Data sources: Y+WK = Yanai et al. (1983) and Warren and Kallemeyn (1989); and as in Table 1.

simple volatility control. To a first approximation, their compositions can be explained by the admixture of a refractory component to a CI-like component. The latter component would be similar to CI-chondrites except for being depleted in relatively volatile elements (*e.g.*, Na, K, Cs, Zn). The refractory component would be rich in Al, Ca, and other elements of similar volatility, perhaps similar to some CAIs in composition.

Trend B inclusions are depleted both in refractory trace-elements and in volatile trace-elements, requiring a more complex history. Their compositions can be explained by the removal of a refractory component from a volatile-depleted, CI-like component. The latter could have been the same CI-like component involved in forming the Trend A inclusions. For the Trend B inclusions, the "missing" refractory component would have to be Mg-rich and olivine-rich, to account for the depletion in Mg relative to Si (Fig. 5a).

The low abundances of siderophile elements for Na-poor inclusions is consistent with the depletion of FeNi-metal in these objects (Fig. 5a). This can be readily explained by a paucity of metal in the precursors out of which the inclusions formed.

This overall model for the formation of Na-poor inclusions is complicated by the fact that local abundance maxima and minima are superposed on the overall abundance patterns. For example, inclusion CB8 has abundances of Al, Ca, and Eu which are greater than would be expected based on volatility alone, producing "spikes" in the CI-normalized abundance pattern (Fig. 5a). This observation, along with a slight LREE-enriched pattern and positive Eu anomaly for this inclusion (Fig. 6a), can be explained by a slight excess of feldspar in the CB8 sample, perhaps caused by an "excess" of feldspar in the precursors out of which CB8 formed. Similarly, LEW-1 contains a prominent depletion of V compared to elements of similar volatility (Fig. 5a). This can be attributed to a deficiency of V-bearing spinel in the precursors out of which this inclusion formed (Ruzicka *et al.*, 1999). Thus, the precursors to the Na-poor inclusions may have consisted of various phases that were not uniformly mixed on the scale of the inclusions (mm to cm).

Refractory trace-element (*e.g.*, REE) data for Na-poor inclusions can be combined with major-element data to further evaluate models for these objects. Figure 7 shows the average CI-normalized REE abundance plotted against the Mg/Si abundance ratio for Na-poor inclusions. The approximate compositions of equilibrium condensates or residues in a system with CI-like overall composition are shown on the diagram, as are the compositions of CAIs and olivine-rich aggregates (OAs). Consistent with the discussion above, Na-poor inclusions could have been derived partly from a precursor similar to CI-chondrites in terms of Mg/Si abundance ratio, but slightly enriched in REE ($\sim$1.2–1.5$\times$CI) (Fig. 7). The REE and Mg/Si data for Na-poor inclusions can be simultaneously explained by the removal or addition of different types of refractory and olivine-rich condensates or residues to this CI-like composition. In particular, Fig. 7 suggests that the precursors to Trend A inclusions LEW-1 and Bo-2 could have formed by the admixture to a CI-like system of a refractory component (REE abundance $\sim$5–10$\times$CI) intermediate in composition to CAIs and OAs. This refractory component is both REE- and

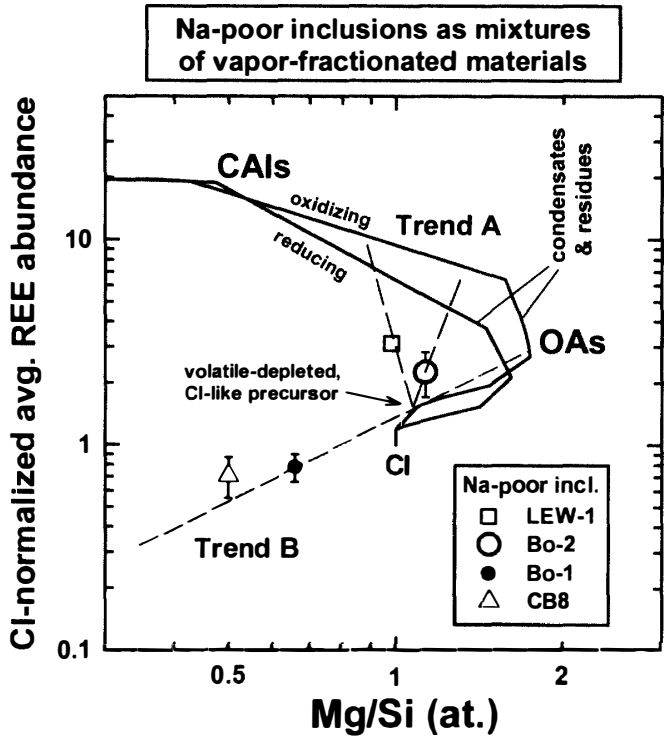

Fig. 7. Mg/Si values and average CI-normalized abundances of rare-earth-elements for Na-poor inclusions compared to the approximate compositions of Ca-Al-rich inclusions (CAIs) and olivine-rich aggregates (OAs) and the calculated compositions of equilibrium condensates or residues in a system with CI-chondrite composition. Trend B inclusions can be produced by the removal of an olivine-rich (OA-like) component and Trend A inclusions can be produced by the addition of a refractory component (intermediate in composition to CAIs and OAs) to a volatile-depleted CI-chondrite composition. The calculated curve for condensates and residues assumes that the CI-normalized REE abundances are equivalent to the CI-normalized abundance of Al. Approximate compositions for CAIs and OAs are from Mason and Taylor (1982). Other data sources, and details associated with the condensate/residue compositions, are as in Fig. 3.

Al-rich, so it is probably not simply anorthite. Similarly, the precursors to Trend B inclusions Bo-1 and CB8 could have formed by the removal from a CI-like system of an Mg-rich (olivine-rich), slightly refractory (REE abundance $\sim 3 \times$ CI) component similar to OAs. Thus, mixing of vapor-fractionated materials can account for the major- and trace-element compositions of Na-poor inclusions in a self-consistent manner.

In contrast, the igneous differentiation models previously proposed for Trend B inclusions Bo-1 (Ruzicka *et al.*, 1995) and CB8 (Bridges *et al.*, 1995) do not easily simultaneously account for the low Mg/Si values and relatively low REE abundances of the inclusions. Fractionation of olivine during igneous differentiation to produce liquids with low Mg/Si values also leads to REE abundances that are enriched, not depleted, relative to chondritic precursors. Moreover, the major-element trend shown by Trend B inclusions in Fig. 5 bears a particular relationship to the predicted compositions of olivine-rich residues or condensates that would

have to be purely coincidental with an igneous differentiation model.

Typical Na-rich inclusions

Typical Na-rich inclusions (AC-1, PV-A, DT4, Y79-2) have relatively uniform abundances of most lithophile elements, ranging from ~1.5 to 2.5×CI (Fig. 5b). Exceptions include a large enrichment in Ba for PV-A and large depletions in P for DT4 and Y79-2, and depletions in Y79-2 of the volatile elements Br and Zn. Inclusion AC-1 has CI-chondrite-like abundances of the siderophile elements, whereas the other inclusions are depleted in these elements. All of the inclusions have low CI-normalized abundances of S (Fig. 5b). REE patterns for these inclusions (Fig. 6b) range from flat (PV-A, Y79-2) to slightly LREE-enriched (AC-1 and DT4); AC-1 also has a positive Eu anomaly.

In contrast to the Na-poor inclusions, there is little evidence for vapor-fractionation in the Na-rich inclusions. In general, the trace-element abundances of these inclusions are consistent with their derivation by impact-melting of whole-rock ordinary chondrites, accompanied in all cases by the loss of sulfide and in most cases by the loss of FeNi-metal. That these inclusions probably formed by shock-melting of ordinary chondrite precursors is in agreement with the conclusions of Fodor *et al.* (1980), Keil *et al.* (1980), Rubin *et al.* (1983a), and Sack *et al.* (1994) for AC-1, PV-A, DT4, and Y79-2, respectively. The LREE-enriched patterns for AC-1 and DT4, and the positive Eu anomaly of AC-1 (Fig. 6b), suggest that the shock-melting process that produced these inclusions may have involved preferential melting of feldspar. This is consistent with the major-element composition trends shown by Na-rich inclusions, which indicate that they are often enriched in an albite component (see above).

Fractionated inclusions

The "fractionated" inclusions (Bar-1, Y75-1, and Y79-1), all from type 6 chondrites, appear to have been chemically modified (Na-metasomatized) and metamorphosed. Bar-1 is an unusually sodic, Na-poor inclusion, and Y75-1 and Y79-1 are two Na-rich inclusions. Evidence for a significant influx of Na into these inclusions from their surroundings (Na-metasomatism) is provided by a radial gradient in Na in all of them (Hutchison *et al.*, 1988; Prinz *et al.*, 1983; Yanai and Kojima, 1993; Sack *et al.*, 1994). Inclusions Y75-1 and Y79-1 may have been metamorphosed *in situ*, as evidenced by similar and low closure temperatures (~710°C) obtained between olivine and spinel in the inclusions and in their hosts (Sack *et al.*, 1994).

Inclusions Bar-1, Y75-1 and Y79-1 have highly fractionated and variable trace-element abundances that are not controlled by volatility (Fig. 5c). Their REE abundances range from LREE-enriched in Bar-1, to "W-shaped" patterns in Y75-1 and Y79-1 (Fig. 6c). All of the inclusions have a positive Eu anomaly (Fig. 6c). The REE pattern of Bar-1 is suggestive of an excess of plagioclase in this inclusion. The distinctive W-shaped REE patterns of Y75-1 and Y79-1 have been attributed to redistribution of the REE into phosphate, which was probably under-represented in the analysis splits, but which is present elsewhere in the inclusions (Nakamura *et al.*, 1994). Such REE redistribution could have occurred either during igneous crystal-

lization, during metamorphic recrystallization, or both. The highly fractionated trace-element compositions of splits of these inclusions could simply reflect non-representative sampling of inclusions that are relatively coarse-grained. Similar W-shaped REE patterns have been observed in some winonaites (*e.g.*, Prinz *et al.*, 1980; Yamamoto *et al.*, 1990; Kimura *et al.*, 1992) and have been attributed to the under-sampling of phosphate in metamorphosed rocks (Kallemeyn and Wasson, 1985; Torigoye *et al.*, 1993).

3.3. Radiometric ages

Radiometric ages have been obtained for several inclusions, primarily utilizing K-Ar and ^{39}Ar-^{40}Ar methods. Figure 8 summarizes the K-Ar and ^{39}Ar-^{40}Ar ages for the inclusions and their chondritic hosts. In this diagram, inclusions Bo-2 and Bar-1 belong to the Na-poor group, and the remaining inclusions belong to the Na-rich group. The most striking feature of the radiometric data is the large variation in age (0.49 Ga to 4.45 Ga) among different inclusions. There is no obvious tendency for the ages to be related to the chemical group or compositions of the inclusions.

However, there is a tendency for the age of an inclusion to be similar to its chondritic host (Fig. 8), although Keil *et al.* (1980) argued that the ^{39}Ar-^{40}Ar age of inclusion PV-A is younger than that of the host (the Plainview polymict, gas-rich breccia). The overall similarity in ages between the inclusions and their hosts suggests that the K-Ar and ^{39}Ar-^{40}Ar ages of the inclusions were reset by shock events. These shock events did not necessarily entail melting the inclusions. In

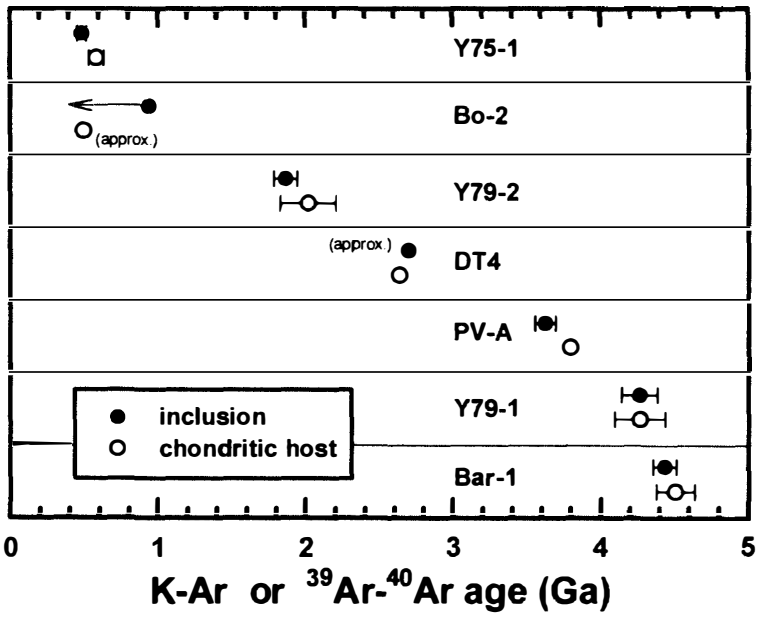

Fig. 8. Plot summarizing K-Ar and ^{39}Ar-^{40}Ar ages for large, igneous-textured inclusions and their ordinary chondrite hosts. Data sources: Y75-1 (Nagao, 1994) and host (Kaneoka et al., 1988; Nakamura et al., 1994); Bo-2 and host (Rubin et al., 1981); Y79-2 and host (Nagao, 1994); DT4 and host (Rubin et al., 1983a); PV-A and host (Keil et al., 1980); Y 79-1 (Nagao, 1994) and host (Nakamura et al., 1994); Bar-1 and host (Hutchison et al., 1988).

other words, with the possible exception of inclusion PV-A, there is little reason to believe that young (<4.4 Ga) K-Ar and ^{39}Ar-^{40}Ar ages for the inclusions represent formation (*i.e.*, shock-melt) ages. Indeed, Rb-Sr and ^{129}Xe data for Y75-1 (Nakamura *et al.*, 1994), which has a 0.49 Ga K-Ar age (Nagao, 1994), implies that the inclusion formed early (~4.56 Ga), and was later degassed in a shock event. Similarly, Rb-Sr and ^{129}Xe data for inclusion Y79-1 (Nakamura *et al.*, 1994) imply that this inclusion formed early (~4.56 Ga) and was later shock-metamorphosed.

3.4. Oxygen-isotopic compositions

Oxygen-isotope data have been obtained for various types of inclusions in ordinary chondrites, including large, igneous-textured inclusions (as defined here) and possibly igneous cristobalite inclusions (CRISPY, CB3, CB5; Olsen *et al.*, 1981; Bridges *et al.*, 1995). Figure 9 compares the oxygen-isotopic compositions of these inclusions to whole-rock ordinary chondrites and to chondrules in these meteorites. The large, igneous-textured inclusions have oxygen-isotope compositions that resemble or bracket those of chondrules and whole-rock chondrites (Fig. 9). Most of the igneous-textured inclusions have $\delta^{18}O$ and $\delta^{17}O$ values which overlap that of H-chondrites and chondrules on the ^{16}O-rich end, but two silica-rich igneous inclusions (Bo-1 and CB8) have considerably higher values, more similar to cristobalite inclusions such as CRISPY (Olsen *et al.*, 1981), CB5, and an inclusion in the Farmington chondrite (Bridges *et al.*, 1995) (Fig. 9). There is no apparent

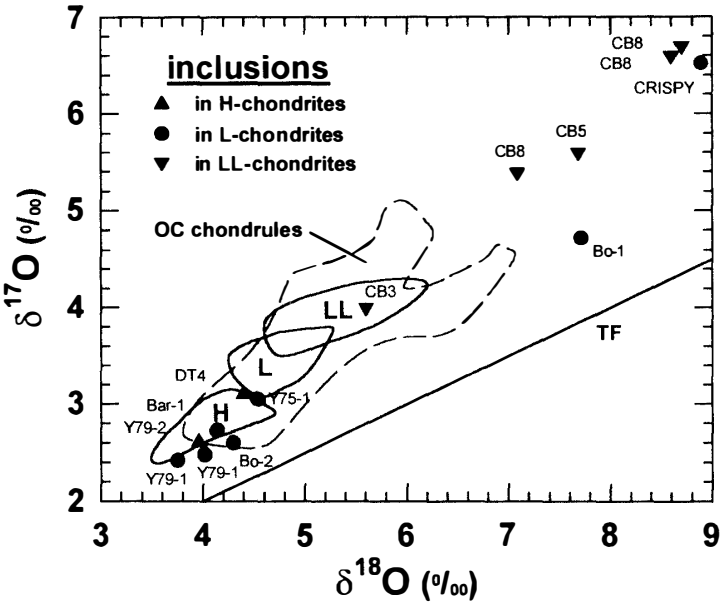

Fig. 9. Oxygen-isotopic compositions of large, igneous-textured inclusions (Y75-1, Y79-2, Bo-1, Bo-2, Bar-1, DT4, multiple splits of CB8 and Y79-1) and cristobalite-rich, possibly igneous inclusions (CRISPY, CB3, CB5) in ordinary chondrites. The fields for H-, L-, and LL- chondrites and for chondrules in ordinary chondrites are from Clayton et al. (1983); data for CB3 and CB5 are from Bridges et al. (1995); data for CRISPY is from Olsen et al. (1981). Other data sources are given in Table 1. TF=terrestrial mass-fractionation line.

relationship between the oxygen-isotopic composition of an inclusion and the host chondrite group in which it occurs (Fig. 9), as is the case for chondrules (Clayton *et al.*, 1983) and for cristobalite inclusions. Bridges *et al.* (1995) previously noted that silica-rich inclusions such as CB8, Bo-1, CRISPY, and CB5 had higher values of $\delta^{18}O$ and $\delta^{17}O$ than other ordinary chondrite materials and suggested that this was caused by preferential exchange of oxygen between the tridymite and cristobalite in silica-rich inclusions and a surrounding, ^{16}O-poor gas. Variable exchange with such a reservoir may have been responsible, in large part, for the variations in oxygen-isotope compositions of ordinary chondrites and chondrules (Bridges *et al.*, 1995, 1998, 1999). The oxygen-isotope data suggest that large, igneous-textured inclusions, chondrules, and cristobalite inclusions in ordinary chondrites could have had similar precursors, or could have been affected by similar processes, or both.

4. Conclusions

Geochemical and isotopic data for large, igneous-textured inclusions in ordinary chondrites suggest that the inclusions formed by the melting of diverse precursors. Some inclusions were metasomatized and metamorphosed, and many appear to have degassed argon in late shock events. Oxygen-isotopic data imply that the precursors and processes that affected inclusions and chondrules in ordinary chondrites were grossly similar. The inclusions can be subdivided into two main chemical groups: Na-rich ($Na/Al > 0.35$ at., with lithophile-element abundances similar to that in ordinary chondrites); and Na-poor ($Na/Al \leq 0.35$, depleted in volatile-lithophile-elements).

The compositions of Na-rich inclusions suggest that they were derived from an ordinary chondrite protolith. These inclusions probably formed by the shock-melting of ordinary chondrites, sometimes involving preferential enrichment of albitic feldspar and usually involving loss of FeNi-metal and sulfide.

In contrast, vapor-fractionation processes appear to have been important in establishing the compositions of Na-poor inclusions. These inclusions could have formed by the melting of vapor-fractionated materials in a system of roughly CI-chondrite composition, which included variable proportions of a refractory component (Al- and REE- rich, similar to CAIs) and an olivine-rich component (Mg-rich and modestly enriched in REE, similar to olivine-rich aggregates). Trend A Na-poor inclusions mainly contain an excess of the refractory component, whereas Trend B Na-poor inclusions mainly contain a deficiency of the olivine-rich component.

These models for large inclusions may also apply to chondrules (Ruzicka *et al.*, 1998). Although large inclusions are comparatively rare, their larger sizes compared to most chondrules make them more amenable to study, and their compositions less susceptible to modification by diffusional exchange with their surroundings. If the two types of objects formed by similar ways, this would imply that chondrules had at least two different types of precursors and origins. Further work on chondrules is needed to test this possibility.

Acknowledgments

The first author (AR) wishes to thank the National Institute of Polar Research for providing accommodations and hospitality while in Tokyo. We also thank John Bridges and Takashi Fujita for helpful reviews, and Allan Patchen for assistance in obtaining microprobe data. This research was supported by NASA grant NAGW-3543.

References

Anders, E. and Grevesse, N. (1989): Abundances of the elements: meteoritic and solar. Geochim. Cosmochim. Acta, **53**, 197–214.

Binns, R. A. (1967): An exceptionally large chondrule in the Parnallee meteorite. Mineral. Mag., **36**, 319–324.

Boctor, N. Z., Bell, P. M., Mao, H. K. and Kullerud, G. (1982): Petrology and shock metamorphism of Pampa del Infierno chondrite. Geochim. Cosmochim. Acta, **46**, 1903–1911.

Bridges J. C. and Hutchison, R. (1997): A survey of clasts and large chondrules in ordinary chondrites. Meteorit. Planet. Sci., **32**, 389–394.

Bridges, J. C., Franchi, I. A., Hutchison, R., Morse, A. D., Long, J. V. P. and Pillinger C. T. (1995): Cristobalite and tridymite-bearing clasts in Parnallee (LL3) and Farmington (L5). Meteoritics, **30**, 715–727.

Bridges, J. C., Franchi, I. A., Hutchison, R., Sexton, A.S. and Pillinger, C. T. (1998): Correlated mineralogy, chemical compositions, oxygen isotope compositions, and sizes of chondrules. Earth Planet. Sci. Lett., **155**, 183–196.

Bridges, J. C., Franchi, I. A., Sexton, A. S. and Pillinger, C. T. (1999): Mineralogical controls on the oxygen isotopic compositions of UOCs. Geochim. Cosmochim. Acta, **63**, 945–951.

Clayton, R. N., Mayeda, T. K., Goswami, J. N. and Olsen, E. J. (1983): Oxygen isotope studies of ordinary chondrites. Geochim. Cosmochim. Acta, **55**, 2317–2337.

Dodd, R. T. and Jarosewich, E. (1976): Olivine microporphyry in the St. Mesmin chondrite. Meteoritics, **11**, 1–20.

Dodd, R. T. and Jarosewich, E. (1982): The compositions of incipient shock melts in L6 chondrites. Earth Planet. Sci. Lett., **59**, 355–363.

Dodd, R. T., Jarosewich, E. and Hill, B. (1983): Petrogenesis of complex veins in the Chantonnay (L 6f) chondrite. Earth Planet. Sci. Lett., **59**, 364–374.

Fodor, R. V., Keil, K. and Jarosewich, E. (1972): The Oro Grande, New Mexico chondrite and its lithic inclusion. Meteoritics, **7**, 495–507.

Fodor, R. V., Prinz, M., Brown, H. G. and Keil, K. (1974): A chondrite with a regolith fragment containing non-chondritic material. Meteoritics, **9**, 337–338 (abstract).

Fodor, R. V. and Keil, K. (1976a): Carbonaceous and noncarbonaceous lithic fragments in the Plainview, Texas, chondrite: Origin and history. Geochim. Cosmochim. Acta, **40**, 177–189.

Fodor, R. V. and Keil, K. (1976b): A komatiite-like lithic fragment with spinifex texture in the Eva meteorite: Origin from a supercooled impact melt of chondritic parentage. Earth Planet. Sci. Lett., **29**, 1–6.

Fodor, R. V., Keil, K., Prinz, M., Ma, M.-S., Murali, A. V. and Schmitt, R. A. (1980): Clast-laden melt-rock fragment in the Adams County, Colorado, H5 chondrite. Meteoritics, **15**, 41–62.

Fredriksson, K., Reid, C. G. R. and Fredriksson B. J. (1981): Grier (b), a "monomict", brecciated chondrite. Meteoritics, **16**, 129–137.

Fujimaki, H., Ishikawa, K. and Aoki, K. (1993): Rb-Sr isotopic study of Yamato-794046 and its inclusion. Papers presented to the 18th Symposium on Antarctic Meteorites, May 31–June 2,

1993. Tokyo, Natl Inst. Polar Res., 24-1 to 24-3.

Fukuoka, T. (1993): Chemistry of the lithic inclusions in Yamato-793241 and -794046 meteorites. Papers presented 18th Symposium on Antarctic Meteorites, May 31–June 2, 1993. Tokyo, Natl Inst. Polar Res., 23-1 to 23-3.

Graham, A. L. (1983): An unequilibrated inclusion in the Romero (H3–4) chondrite. Meteoritics, **18**, 51–61.

Hutchison, R., Williams, C. T., Din, V. K., Clayton, R. N., Kirschbaum, C., Paul, R. L. and Lipschutz, M. E. (1988): A planetary, H-group pebble in the Barwell, L6, unshocked chondritic meteorite. Earth Planet. Sci. Lett., **90**, 105–118.

Jarosewich, E. (1990): Chemical analyses of meteorites: A compilation of stony and iron meteorite analyses. Meteoritics, **25**, 323–337.

Kallemeyn, G. W. and Wasson, J. T. (1985): The compositional classification of chondrites: IV. Ungrouped chondritic meteorites and clasts. Geochim. Cosmochim. Acta, **49**, 261–270.

Kaneoka, I., Takaoka, N. and Yanai, K. (1983): ^{40}Ar-^{39}Ar analyses of Yamato-75097 (L6) chondrite from Antarctica. Proc. NIPR Symp. Antarct. Meteorites, **1**, 206–214.

Keil, K., Fodor, R. V., Starzyk, P. M., Schmitt, R. A., Bogard, D. D. and Husain, L. (1980): A 3.6-b.y.-old impact melt rock fragment in the Plainview chondrite: Implications for the age of the H-group chondrite parent body. Earth Planet. Sci. Lett., **51**, 235–247.

Kimura, M., Tsuchiyama, A., Fukuoka, T. and Iimura, Y. (1992): Antarctic primitive achondrites, Yamato-74025, -75300, and -75305: Their mineralogy, thermal history, and the relavance to winonaite. Proc. NIPR Symp. Antarct. Meteorites, **5**, 165–190.

MacPherson, G. J., Wark, D. A. and Armstrong, J. T. (1988): Primitive material surviving in chondrites: Refractory inclusions. Meteorites and the Early Solar System, ed. by J. F. Kerridge and M. S. Matthews. Tucson, Univ. Arizona Press, 746–807.

Mason, B. and Taylor, S. R. (1982): Inclusions in the Allende meteorite. Smithson. Contrib. Earth Sci., **25**, 30 p.

Mayeda, T. K., Clayton, R. N. and Yanai, K. (1987): Oxygen isotopic compositions of several Antarctic meteorites. Mem. Natl Inst. Polar Res. Spec. Issue, **46**, 144–150.

Nagao, K. (1994): Noble gases in hosts and inclusions from Yamato-75097 (L6), -793241 (L6) and -794046 (H5). Proc. NIPR Symp. Antarct. Meteorites, **7**, 197–216.

Nakamura, N., Yanai, K. and Matsumoto, Y. (1984): Unique clasts with V-shaped REE pattern in L6 chondrites. Meteoritics, **19**, 278–279 (abstract).

Nakamura, N., Morikawa, N., Hutchison, R., Clayton, R. N., Mayeda, T. K., Nagao, K., Misawa, K., Okano, O., Yamamoto, K., Yanai, K. and Matsumoto, Y. (1994): Trace-element and isotopic characteristics of inclusions in the Yamato ordinary chondrites Y-75097, Y-793241 and Y-794046. Proc. NIPR Symp. Antarct. Meteorites, **7**, 125–143.

Olsen, E. J., Mayeda, T. K. and Clayton, R. N. (1981): Cristobalite-pyroxene in an L6 chondrite: Implications for metamorphism. Earth Planet. Sci. Lett., **56**, 82–88.

Prinz M., Waggoner, D. G. and Hamilton, P. J. (1980): Winonaites: A primitive achondritic group related to silicate inclusions in IAB irons. Proc. Lunar and Planet. Sci. 11th, 902–904.

Prinz, M., Nehru, C. E., Weisberg, M. K. and Delaney, J. S. (1984): H chondritic clasts in a Yamato L6 chondrite: Implications for metamorphism. Meteoritics, **19**, 292–293 (abstract).

Prinz, M., Weisberg, M. K. and Nehru, C. E.. (1988): Gunlock, a new Type 3 ordinary chondrite with a golfball-sized chondrule. Meteoritics, **23**, 297 (abstract).

Rubin, A. E., Keil, K., Taylor, G. J., Ma, M.-S., Schmitt, R. A. and Bogard, D. D. (1981): Derivation of a heterogeneous lithic fragment in the Bovedy L-group chondrite from impact-melted porphyritic chondrules. Geochim. Cosmochim. Acta, **45**, 2213–2228.

Rubin, A. E., Scott, E. R. D., Taylor, G. J., Keil, K., Allen, J. S. B., Mayeda, T. K., Clayton, R. N. and Bogard, D. D. (1983a): Nature of the H chondrite parent body: Evidence from the Dimmitt breccia. Proc. Lunar Planet. Sci. Conf., 13th, Pt. 2, A741–A754 (J. Geophys. Res., 88 Suppl.).

Rubin, A. E., Rehfeldt, A., Peterson, E., Keil, K. and Jarosewich, E. (1983b): Fragmental breccias and

the collisional evolution of ordinary chondrite parent bodies. Meteoritics, **18**, 179–196.

Ruzicka, A., Kring D. A., Hill, D. A., Boynton, W. V., Clayton, R. N. and Mayeda, T. K. (1995): Silica-rich orthopyroxenite in the Bovedy chondrite. Meteoritics, **30**, 57–70.

Ruzicka, A., Snyder, G. A. and Taylor, L. A. (1998): Mega-chondrules and large, igneous-textured clasts in Julesberg (L3) and other ordinary chondrites: Vapor-fractionation, shock-melting, and chondrule formation. Geochim. Cosmochim. Acta, **62**, 1419–1442.

Ruzicka, A., Jerde, E. A., Snyder, G. A. and Taylor, L. A. (1999): A large, igneous-textured inclusion containing co-existing enstatite and ferroan olivine in the LEW 86018 (L3.1) chondrite. Lunar and Planetary Science XXX. Houston, Lunar Planet. Inst., Abstract #1502 (CD-ROM).

Sack, R. O., Ghiorso, M. S., Wang, M.-S. and Lipschutz, M. E. (1994): Igneous inclusions from ordinary chondrites: High temperature cumulates and a shock melt. J. Geophys. Res., **99**, 26029–26044.

Stöffler, D., Keil, K. and Scott, E. R. D. (1991): Shock metamorphism of ordinary chondrites. Geochim. Cosmochim. Acta, **55**, 3845–3867.

Torigoye, N., Yamamoto, K., Misawa, K. and Nakamura, N. (1993): Compositions of REE, K, Rb, Sr, Ba, Mg, Ca, Fe, and Sr isotopes in Antarctic "unique" meteorites. Proc. NIPR Symp. Antarct. Meteorites, **6**, 100–119.

Warren, P. H. and Kallemeyn, G. W. (1989): Allan Hills 84025: The second Brachinite, far more differentiated than Brachina, and an ultramfic achondrite clast from L chondrite Yamato 75097. Proc. Lunar Planet. Sci. Conf., 19th, 475–486.

Weisberg, M. K., Prinz, M. and Nehru, C. E. (1988): Macrochondrules in ordinary chondrites: Constraints on chondrule-forming processes. Meteoritics, **23**, 309–310 (abstract).

Wood, J. and Hashimoto, A. (1993): Mineral equilibrium in fractionated nebular systems. Geochim. Cosmochim. Acta, **57**, 2377–2388.

Yamamoto, K., Nakamura, N., Misawa, K., Yanai, K. and Matsumoto, Y. (1990): Lithophile trace element abundances in Antarctic unique meteorites and in unique clasts from L6 chondrites. Papers presented to the 15th Symposium on Antarctic Meteorites, May 30–June 1, 1990. Tokyo, Natl Inst. Polar Res., 97–98.

Yanai, K. and Kojima, H. (1987): Photographic Catalog of the Antarctic Meteorites. Tokyo, Natl Inst. Polar Res., 298 p.

Yanai, K. and Kojima, H. (1993): General features of some unique inclusions in Yamato ordinary chondrites. Papers presented to the 18th Symposium on Antarctic Meteorites, May 31–June 2, 1993. Tokyo, Natl Inst. Polar Res., 19-1 to 19-4.

Yanai, K., Matsumoto, Y. and Kojima, H. (1983): A Brachina-like inclusion in the Yamato-75097 L6 chondrite: A preliminary examination. Mem. Natl Inst. Polar Res., Spec. Issue, **30**, 29–35.

(Received July 29, 1999; Revised manuscript received December 9, 1999)